1976

Evidence for an isovector octupole resonance at 28.4 MeV and other Giant Resonances in 238U

Houk, W.A.

Monterey, California. Naval Postgraduate School

NAVAL POSTGRADUATE SCHOOL

Monterey, California

Evidence for an Isovector Octupole Resonance at 28.4 MeV and other Giant Resonances in ^{238}U*

W.A. Houk, R.W. Moore, F.R. Buskirk and R. Pitthan

Department of Physics and Chemistry

* Supported in part by the National Science Foundation and the Naval Postgraduate School Research Foundation

The deformed, fissionable nucleus ^{238}U was studied with inelastic scattering of 87.5 MeV electrons between 5 and 40 MeV excitation energy, at scattering angles of 45^{o}, 60^{o}, 75^{o} and 90^{o}. Resonance cross sections extracted from the spectra were compared with DWBA calculations using the Tassie (Goldhaber-Teller) model. The results agree with the known positions, widths and cross sections of the two branches of the giant dipole resonance at E_x = 10.9 MeV and 14.0 MeV, thus confirming the validity of the evaluation method. In addition, isoscalar and isovector E2 resonances and an isovector E3 resonance were found at 9.9 MeV (Γ = 2.9), 21.5 MeV (Γ = 4.9) and 28.4 MeV (Γ = 8.1), exhausting 40%, 50% and 90% of the respective EWSR. Although isospin cannot be determined from (e,e'), ΔT assignments were based on microscopic and macroscopic considerations.

Electroexcitation ^{238}U(e,e'), E_o = 87.5 MeV, measured $d^2\sigma/d\Omega dE_x$, deduced giant resonance parameters B(Eλ), Γ, E_x, and sum rule exhaustion.

1. INTRODUCTION

In recent years, there has been a renewed interest in the structure of the nuclear continuum. This interest has been stimulated by the discovery of numerous isoscalar and isovector resonances of various multipolarities above particle threshold (giant resonances), which had been predicted by Bohr and Mottelson[1]. Inelastic scattering was not used to identify and locate giant resonances in medium-heavy and heavy nuclei until about 1970, when both magnetic dipole and electric quadrupole giant resonances were identified in N = 82 nuclei[2]. This was followed by verification through reevaluation of older proton experiments[3]. Since that time, several groups have been investigating nuclei of interest. This experiment is the first (e,e') investigation of a fissionable, deformed nucleus in the excitation range up to 40 MeV.

Investigation of ^{238}U by photo nuclear methods has a long tradition[4]. More recently Bar-noy and Moreh[5] utilized thermal neutron capture, Gurevich et al.[6] employed bremsstrahlung beams, and Veyssière, et al.[7] and Caldwell, et al.[8] used quasi monochromatic photons. The four above research groups located the maxima of the two branches of the giant dipole resonance in ^{238}U at excitation energies of about 10.9 and 14.0 MeV.

In proton scattering on ^{238}U, a "bumplike" resonance was found by Lewis and Horen in the 10-13 MeV excitation energy range which was interpreted as a quadrupole resonance[9]. Approximately 85% of the isoscalar sum rule was exhausted.

Wolynec, Martins and Moscati[10] have used the ^{238}U (e,α) ^{234}Th reaction to investigate the giant quadrupole resonance (GQR). Approximately 50% of the isoscalar energy-weighted sum rule (EWSR) was exhausted by a Breit-Wigner shaped resonance at 8.9 MeV with Γ = 3.7 MeV.

The present experiments were undertaken to measure the excitation energies and strengths of the quadrupole modes of a deformed fissionable nucleus by inelastic electron scattering. The techniques employed were similar to those used in earlier (e,e') experiments with ^{208}Pb, ^{197}Au, ^{165}Ho, ^{140}Ce and ^{90}Y,[11-14] so that comparisons between the nuclei could be made without variations from differing methods of evaluation. Special difficulties arise in the evaluation of the ^{238}U spectra because the radiation tail, which has a strength appr. proportional to Z^2, is extremely large. Furthermore, because the nucleus is deformed, the resonances are possibly split, as has been observed for the dipole state, or at least broadened and tend to be more spread out than in spherical nuclei[13].

On the other hand, though large, the radiative background in (e,e') is well understood and, although no rigorous treatment is possible yet, due to practical improvements the calculations account for virtually all the radiative background. It is especially to be noted that the two regions where one knows the background experimentally (namely between low-lying isolated levels and above the giant resonance region, that is, above 40 to 50 MeV excitation energy), are reproduced within a few percent.

Our evaluation is sensitive to resonant structure; more continuous cross sections, e.g., from the tail of the quasi elastic peak, would not be seen with our method, because it would change mainly the constant and linear term in our background function (see below).

2. EXPERIMENTAL DETAILS

87.5 MeV electrons from the NPS 120 MeV electron LINAC were scattered by self supporting ^{238}U foils at scattering angles of 45^{o}, 60^{o}, 75^{o} and 90^{o}, thus using the variation of the momentum transfer with angle to investigate the multipolarity of the giant resonances. A wider spread of angles was not necessary because the maxima of E1 to E4 form factors are included in this range. After scattering, the electrons were detected by a counter ladder in the focal plane of a 16" magnetic spectrometer. The general set-up of the NPS linear accelerator has been recently described in more detail[14].

Samples of 99.9% enriched ^{238}U were obtained from Ventron Corp. and Research Organic/Inorganic Corp. and rolled to 0.004 inches for the 90^{o} scattering angle, 0.002 inches for the 60^{o} and 75^{o} scattering angles, and 0.001 inches for the 45^{o} scattering angle. Using three different target thicknesses made it possible to optimize count rates while achieving the required statistical accuracy.

3. EVALUATION

The inelastic cross sections were measured relative to the elastic ones. The latter, in turn, were calculated with a phase shift code[15] using the Fermi ground state charge distribution parameters c = 6.805 fm and t = 2.66 fm. These parameters which are from elastic electron scattering were taken from the compilation by De Jager, et al.[16]. The inelastic reduced transition probabilities were calculated with the DWBA program of Tuan et al.[17]. The parameters of the transition charge density, as defined by Ziegler and Peterson[18], were $c_{tr}/c = 1$ and $t_{tr}/t = 1$ for the E2 and E3 calculations. Values of c_{tr}/c equal to 1.24 and 0.90 were used for the GDR corresponding to the long and short axes, respectively, of the deformed uranium nucleus. These values were calculated in the following way: The equivalent radius, r_{eq}, is defined as the radius of the sphere which has the same volume as the ellipsoid defined by the short and long axis. The values of c_{tr} were calculated by multiplying the ground state charge density parameter, c, by the ratio of a/r_{eq} and b/r_{eq}, respectively; t_{tr} was assumed to be equal to t.

In other words, a strict hydrodynamic model was used for the transition charge density $\rho_{tr}(r)$. This strict model leads to $\rho_{tr}(r) \sim r^{\lambda-1} d\rho_{o}(r)/dr$, an expression derived by both Goldhaber-Teller and Tassie models (for a more detailed discussion see, e.g., Ref. 14 and 19). For many low-lying levels it has been found that parameters of the hydrodynamical model have to be changed to achieve agreement between

DWBA calculations and experiments. The model dependency, however, was found to be small if both c_{tr} and t_{tr} were allowed to vary.[18] No such changes have been found necessary for giant resonances, which may be not too surprising, because the continuum excitations of nuclear matter are the hydrodynamical modes of the nucleus. The attempt to fit the transition charge densities (that is c_{tr} alone) to the experimental data at higher momentum transfer ($q \gtrsim 0.8$ fm^{-1}) in the case of ^{181}Ta leads to a c_{tr} which is approximately 20% smaller than that of the hydrodynamical model[19]. The transition strengths found that way are a factor of 2 to 3 smaller than these from either other (e,e') experiments or from other reactions in comparable nuclei. The deviation between DWBA calculations and experiment in ^{181}Ta might be due to non-resonant higher multipole strength instead to a failure of the hydrodynamical model.

Since there are many more shell model configurations available for E4 and higher multipolarities than for E3 and E2, a wider distribution of strength may be expected, supported by the fact that no continuum states with $\lambda \geq 4$ have been observed with certainty up to now. Further support for the application of the strict hydrodynamic model to giant resonances comes from the very good agreement in strength extracted that way from (e,e'), (γ,n) and inelastic hadron scattering.

The inelastic spectra were evaluated using a least square line shape fitting program, as described recently[14], in which the resonances and the background are fit simultaneously. The largest part of the total background is the

elastic radiation tail which is caused by photon emission before, during and after the scattering event, plus energy straggling and ionization. The radiation tail was calculated using the Born approximation formulas of Ginsberg and Pratt[20] but substituting the actual elastic cross section, computed with the phase shift code of Fischer and Rawitscher[15].

In addition to the radiation tail, the experimental background, consisting of general room background and of electrons scattered by the targets and subsequently rescattered by the spectrometer walls, had to be taken into account. The total background was found to be well described with a three parameter function:

$$BGR(E_f) = P_1 + P_2/E_f + P_3 \cdot RT\ (E_f)$$

or

$$BGR(E_f) = P_1 + P_2 \cdot (E_f - E') + P_3 \cdot RT\ (E_f),$$

where the P_i are fitting parameters, E_f is the energy of the outgoing electron, E' is the center energy of the fitting range, and RT is the radiation tail. The parameter P_3 turned out to be close to one, which shows that little scaling of the calculated radiation tail was necessary. A more detailed discussion can be found in Ref. 14. There was no difference between the results obtained using the above two background functions. The second function was used in the final analysis of all spectra. In addition, a bump from instrumental scattering (ghost peak) at 6.5 MeV had to be subtracted[14].

Three alternate criteria were used for placing a resonance in the spectrum: (1) the observation of the resonance peaking above the flat expanse of the radiation tail and background, (2) the knowledge of resonances found by photonuclear and photofission experiments[5-8], (3) the necessity to add a resonance to achieve a consistent overall fit. In the case of uranium, it is difficult to use the first criterion for reasonable placement. As can be seen in the inelastic spectrum for 75° (Figure 1), very few of the collective states are visible to the naked eye. It is only after the subtraction of the radiation tail and continuous spectrum due to bremsstrahlung that the spectrum begins to exhibit the structure of the giant multipole resonances.

All lines were fitted using a Breit-Wigner line shape. This choice was based on a recent study[21] in which Gaussian, Lorentz and Breit-Wigner line shapes were compared for photonuclear giant resonances, and where the latter form gave the best results.

It is customary to express giant resonance cross sections as fractions of the electromagnetic sum rules. This is particularly appropriate for electron scattering, because here the sum rules only depend on the nuclear charge distribution of the ground state. In this paper the isoscalar sum rule for $\lambda > 1$

$$S(E\lambda,\Delta T = 0) = \frac{Z^2}{8\pi AM_p}\frac{\lambda(\lambda+1)^2\hbar^2}{}\langle R^{2\lambda-2}\rangle$$

was used, where M_p is the mass of the proton and $\langle R^{2\lambda-2}\rangle$ the $(2\lambda-2)$ - moment of the ground state charge distribution of the nucleus[22]. This sum rule does not account for interference terms between isoscalar and isovector excitations. Isoscalar and isovector sums are related by

$$S(E\lambda,\ \Delta T = 1) = S(E\lambda,\ \Delta T = 0)(N/Z).$$

The energy-weighted isovector sum rule for the electric dipole resonance is[22]

$$S(E1) = \frac{9}{8\pi M_p}\hbar^2\ (NZ/A)\ .$$

The energy-weighted sum rules for ^{238}U, calculated with $\langle R^2\rangle^{1/2} = 5.730$ fm and $\langle R^4\rangle^{1/4} = 6.124$ fm, which in turn were calculated by numerical integration of the ground state charge distribution, are $S(E2,\ \Delta T = 1) = 1.53 \times 10^5$ MeV fm^4, $S(E2,\ \Delta T = 0) = 9.64 \times 10^4$ MeV fm^4, $S(E3,\ \Delta T = 1) = 1.93 \times 10^7$ MeV fm^6, and $S(E1,\ \Delta T = 1) = 837.8$ MeV fm^2.

4. RESULTS

4.1 General

A spectrum taken at a scattering angle of 75^{o} is snown in Figure 1. The background has not been subtracted and the cross section has not been corrected for the constant momentum dispersion of the magnetic spectrometer. Figure 2 shows all the spectra taken after subtraction of the total background. All of these spectra show the split GDR at 11 and 14 MeV, conforming to photonuclear data. In addition, structure is evident at approximately 21 MeV and 29 MeV. Other structure at 10 and 17 MeV is not visible in the spectra but the assumption of resonances at this energy was necessary to achieve a consistent analysis.

Past giant resonance research with other nuclei has provided an initial designation for the visible resonances. The GDR has already been mentioned; in terms of $A^{-1/3}$, the excitation energy of the 21 MeV resonance is in agreement with that of the E2($\Delta T = 1$)GR[12]. The 29 MeV line is lower in energy compared to the value of 195 $A^{-1/3}$ which was found for a resonance-like structure in ^{197}Au and ^{208}Pb[12].

4.2 The Isoscalar Giant Quadrupole Resonance

Figure 3 shows that the resonance found at 9.9 ± 0.2 MeV with a width of $2.9 \begin{smallmatrix} + 0.8 \\ - 0.4 \end{smallmatrix}$ MeV conforms to an E2 DWBA momentum transfer. The reduced transition probability of 3700 ± 400 fm^4 corresponds to 40% of the energy-weighted sum rule. Excitation energy, width and strength (Table 1) are in fair agreement with the (e,α) measurements[10].

Agreement is not good with the excitation energy of 10-13 MeV and strength of 85% EWSR from (p,p') experiments[9]. Compared to the systematics of the E2 ($\Delta T = 0$) strength in heavy nuclei[11-14], only half of the expected strength has been found. The ghost peak may have affected results for this line, which has the lowest excitation energy of those evaluated and is thus closest to it.

On the other hand it is remarkable that the strength found for the isovector E2 (see D, below) is also only 50% of the sum rule. It is not clear whether or not this result is due to fission.

4.3 The Giant Dipole Resonance

Deformation of nuclei shows up most clearly in the giant dipole resonance. The giant dipole state of the nucleus splits because a nuclear vibration along the short axis has a higher frequency, and one in the direction of the long axis has a lower frequency[7]. Due to the increasing number of sublevels, the splitting is not so definite for multipole resonances higher than the GDR, but a broadening has been observed[13,23,24]. The two branches of the GDR in ^{238}U were evaluated with the Goldhaber-Teller model using two different transition charge distributions corresponding to the long and short axes of the deformed nucleus. The Steinwedel-Jensen model was also investigated, but did not describe the measured cross section, which is in agreement with results[14] from ^{89}Y .

Danos[25] gave the relation between the energies, E_a and E_b, of the two branches of the GDR as

$$\frac{E_a}{E_b} = 0.911 \frac{a}{b} + 0.089 ,$$

where a and b are the lengths of the long and short axes of the deformed spheroid. He also gave the relationship between the reduced transition probabilities (B-values) of the long and short axis resonances as 1:2. This ratio has been proven to be approximately right in past photonuclear work.

The GDR associated with the long axis of the nucleus was found to be at 10.75 ± 0.25 MeV with Γ = 3.2 ± 0.4 MeV. As seen in Table 2, this is a slightly lower energy than found in either the (γ,n) results[6-8] or the (γ,γ') experiment[5]. The results of the past and present work agree within errors. The curve shown in Figure 4 was normalized to the photonuclear[6] reduced transition probability of 30.4 fm^2 to show how well the results compare with the known photonuclear information.

Associated with the short axis of the nucleus is the GDR found at 13.95 ± 0.25 MeV with $\Gamma = 4.5 \begin{smallmatrix} + 0.2 \\ - 0.3 \end{smallmatrix}$ MeV. Table 2 contains the resumé of all work done with this resonance. Figure 5 is also normalized to the photonuclear transition probability of Gurevich, et al. (49.0 fm^2)[6]. This agreement shows that the evaluation method used is basically correct. The slightly lower excitation energy may be due to the different dependence of the resonance on the excitation energy in (γ,n) and (e,e')[21].

4.4 The Isovector Giant Quadrupole Resonance

Although some work has been done on the isoscalar GQR region[9] in ^{238}U, there has not been any investigation in the 20-40 MeV region. The measurements here show two resonances in this excitation energy range. The relative cross section for the one at 21.6 ± 0.6 MeV is shown in Figure 6 and compared to the E2 and E3 DWBA cross sections. The result clearly favors E2. The excitation energy found corresponds to 133 $A^{-1/3}$ MeV which agrees well with the value 130 $A^{-1/3}$ MeV found to describe the isovector E2 GR in both spherical[12] and deformed[13] nuclei. Similarly the width, 5.0 ± 0.6 MeV, but not the strength, (50 ± 8)% EWSR, agrees with the results in ^{208}Pb[12] and ^{165}Ho[13]. This resonance was not seen in the 45° spectrum but the GQR should be very small at this angle. The line and arrow drawn in Figure 6 indicate the maximum cross section of the GQR that the curve fitting program would accept, maintaining $\chi^2 \leq 1.0$. It is interesting to note that both E2 resonances ($\Delta T = 0$ and $\Delta T = 1$) in ^{238}U exhaust only half of the appropriate sum rules.

4.5 The Isovector Giant Octupole Resonance

The E3 strength is more widely distributed and more difficult to locate than the quadrupole strength since the shell model allows both $1\hbar\omega_o$ and $3\hbar\omega_o$ transitions for octupole excitations of the continuum but only $2\hbar\omega_o$ for quadrupole excitations. A resonance comparing favorably with an E3 DWBA cross section (Figure 7) was found at 28.4 ± 1.2 MeV with Γ = 8.1 ± 1.1 MeV and exhausting (90 ± 15)% of the EWSR.

This excitation energy corresponds to 176 $A^{-1/3}$ MeV; thus it is lower than the 195 $A^{-1/3}$ MeV predicted for spherical heavy nuclei[26], but in qualitative agreement with the corresponding resonance in the deformed ^{165}Ho. Based on its excitation energy, strength and angular distribution this resonance should be classified as the E3 $3\hbar\omega_o$ ($\Delta T = 1$) resonance.

4.6 Other Structure

The 45° and 90° spectra (Figure 2) show another structure which has not been identified or discussed thus far. Taken as a resonance, the excitation energy is 17.0 ± 1.8 MeV and the width is 3.9 ± 1.8 MeV. Although the resonance energy of 106 $A^{-1/3}$ MeV closely compares to the ($3\hbar\omega_o$) isoscalar E3 resonance predicted by the shell model[27], it does not follow the angular distribution for an E3 cross section. Further investigation is needed to state the multipolarity and strength of this structure. The momentum transfer dependence could be explained with a M1 + E3 assignment, but since the measurements were not extended to backward angles, no definite assignment can be made.

5. SUMMARY AND CONCLUSIONS

The excitation energy range between 5 and 40 MeV was measured in ^{238}U and the spectra were analyzed for resonant structure. The data are in principal agreement with other experiments and microscopic and macroscopic theoretical considerations, at least concerning the excitation energy and total width. Table 3 is a compilation of the results of this experiment.

The following points should be emphasized:

1. When the energy is expressed in $A^{-1/3}$ units, the resonance at 28.4 (176 $A^{-1/3}$) MeV has lower excitation energy in ^{238}U than previously reported in spherical nuclei. For ^{197}Au and ^{208}Pb, a resonance was found at 33.5 MeV and 33 MeV respectively[12] and thus followed an 195 $A^{-1/3}$ MeV rule. Moore, et al.[13] reported a resonance at 34 MeV in ^{165}Ho which would correspond to 186 $A^{-1/3}$ MeV. As both ^{238}U and ^{165}Ho are deformed nuclei, it may be concluded that the deformation lowers the excitation energy when compared to results from spherical nuclei.

2. The isoscalar E2 resonance has a lower excitation energy than previously reported in ^{238}U. In addition, only 40% of the isoscalar EWSR is exhausted.

3. Both parts of the GDR, split due to deformation, conform to the photonuclear data.

4. The isovector GQR is in agreement with the 130 $A^{-1/3}$ MeV rule found from other nuclei. It accounts for only half of the appropriate sum rule, which is similar to the result for the $\Delta T = 0$ E2 state.

The low E2 strength leads to the question whether the strict hydrodynamical model which has been successful in describing the data in non-fissionable nuclei can also be applied to ^{238}U for quadrupole excitations, or if the quadrupole strength is shifted to lower energy or spread out in a non-resonant way. Although this problem will need more experimental work, one may reason that for a fissionable nucleus the rms-radius for the charge distribution in the excited state may be expected to be greater than the one calculated from the hydrodynamical model. A study of Ref. 18 then shows that such an assumption leads to a greater sum rule exhaustion, but still does not explain why this effect should be very strong for E2 oscillations, but not noticeable for E1 excitations.

The comparison of Table 3 with the table in Ref. 12 shows that the widths found for the resonances are systematically, but only slightly greater than the widths in ^{208}Pb. While the large deformation of ^{238}U leads one to expect a large broadening, the viscosity model of Auerbach and Yeverechyahu[28] shows that the width decreases with increasing mass; thus the combined effect is compatible with our data.

Table 1

Comparison of known results for the E2, $\Delta T = 0$ resonance from various reactions.

Table 2

Comparison of results for the GDR from various experiments.

Table 3

Results for all resonances evaluated. The errors were estimated from the maximum and minimum values for excitation energy, width and strength that fit into the spectrum with $\chi^2 < 1.1$. The Γ_γ^0 and single particle units (SPU) are defined by S. J. Skorka et al. (Nucl. Data A2, 347 (1966)).

Table 1

Reference	E_x (MeV)	Γ(MeV)	R(%) [a]	Reaction
9	10 - 13	---	85	(p,p')
10	8.9 ± 0.3	3.7 ± 1.2	50	(e,α)
This work	9.9 ± 0.2	$2.9^{+0.8}_{-0.4}$	40	(e,e')

a) $R = E_x \cdot B(E2)/EWSR(E2,\Delta T=0)$

Table 2

Ref.	Reaction	Long Axis E_x (MeV)	Long Axis Γ(MeV)	Long Axis B(fm^2)	Short Axis E_x (MeV)	Short Axis Γ(MeV)	Short Axis B(fm^2)
7	(γ,n)	10.96±0.09	2.90±0.14	31.1	14.04±0.13	4.53±0.13	46.5
5	(γ,γ')	10.95±0.06	2.62±0.19	28.0	14.00±0.68	4.53±0.20	48.3
8	(γ,n)	10.80	2.44	28.2	13.85	5.12	65.5
6	(γ,n)	10.97±0.13	2.99±0.48	30.4	14.25±0.18	5.10±0.63	49.0
This work	(e,e')	10.75±0.25	$3.2^{+0.4}$	28.1	13.95±0.25	$4.5^{+0.2}_{-0.3}$	49.2

Table 3

E_x (MeV)	Eλ	ΔT	E_x ($A^{-1/3}$)	Γ (MeV)	B(Eλ) ($fm^{2\lambda}$)	Γ_γ^o(eV)	SPU	R(%)[a]
9.9±0.2	E2	0	62	$2.9^{+0.8}_{-0.4}$	3.7×10^3	56	17.4	40±10
10.8±0.3	E1(long)	1	67	3.2±0.4	3.0×10^1	$1.3 \cdot 10^4$	5.3	36± 4
13.9±0.3	E1(short)	1	86	$4.5^{+0.3}_{-0.4}$	4.9×10^1	$4.6 \cdot 10^4$	9.8	83± 8
21.6±0.7	E2	1	133	5.0±0.6	3.6×10^3	$2.7 \cdot 10^3$	17.1	50± 8
28.4±1.2	E3	1	176	8.1±1.1	6.2×10^5	$5.4 \cdot 10^2$	78.0	90±15

a) $R = E_x \cdot B(E\lambda)/EWSR(E\lambda,\Delta T)$

Figure 1 Spectrum of 87.5 MeV electrons scattered inelastically from ^{238}U at 75°. Note the suppressed scale; the resonant cross section is only a small fraction of the underlying radiation tail. The raising line at the very left is due to the tail of the ghost peak. The cross section has not been corrected for the constant dispersion of the magnetic spectrometer.

Figure 2 87.5 MeV electrons scattered inelastically from ^{238}U at 45°, 60°, 75° and 90°. The fitted background consisting of radiation tail, general room background and instrumental scattering has been subtracted. The relative change in peak-height of various resonances to each other indicates that different multipolarities contribute.

Figure 3 Comparison of experimental and DWBA cross sections (divided by the Mott cross section) for the resonant structure at 9.9 MeV shows the E2 character of this state.

Figure 4 Comparison of experimental and DWBA cross section for the resonance at 10.7 MeV. The calculations were done using the Goldhaber-Teller model, modified as described in the text to take into account the deformation of the ^{238}U nucleus, assuming that this resonance is due to the oscillation along the long axis. The Steinwedel-Jensen model was

used too, but described neither the momentum transfer dependence nor the photon point ((γ,n) - data) correctly.

Figure 5 Similar to Figure 4, but for the resonance at 13.9 MeV (short axis).

Figure 6 Comparison of experimental and DWBA cross sections, calculated using the Goldhaber-Teller model for the resonance at 21.6 MeV, favors an E2 assignment (ΔT = 1) for this state. The black dot with arrow indicates that no resonance has been seen at this energy, but that an upper limit of 1 standard deviation in peak-height is in agreement with the data.

Figure 7 Similar to Figure 6, but for resonance at 28.4 MeV. The comparison favors an E3 assignment.

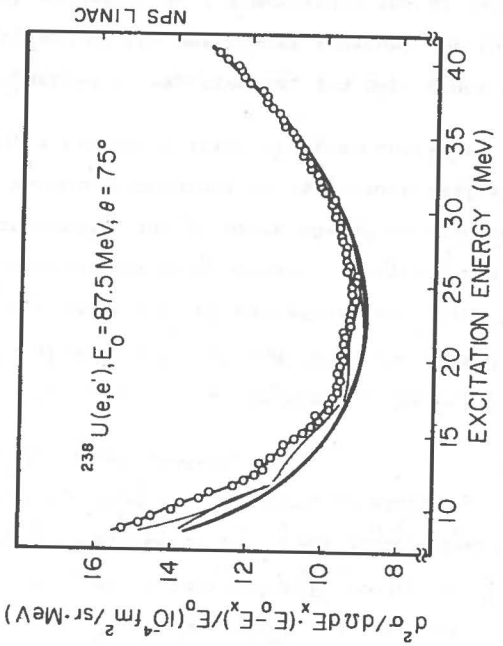

FIGURE 1

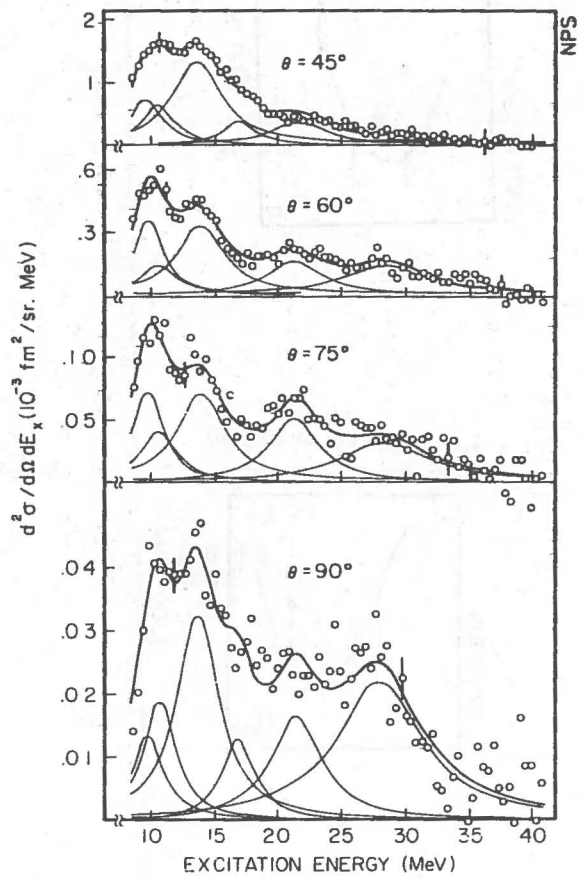

FIGURE 2

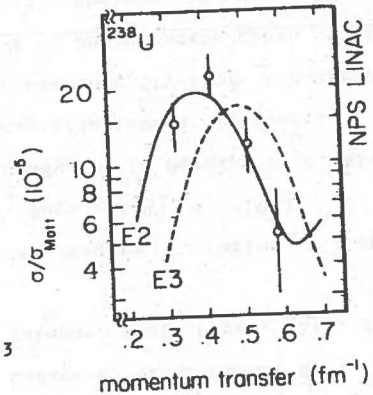

FIGURE 3

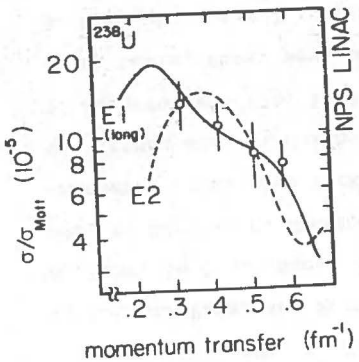

FIGURE 4

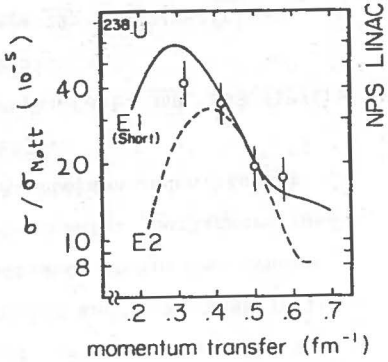

FIGURE 5

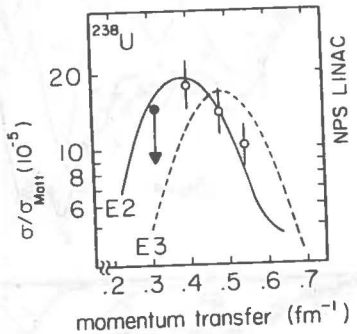

FIGURE 6

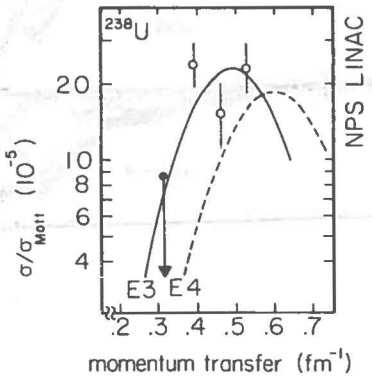

FIGURE 7

References

1. B. R. Mottelson, in "Int. Conf. on Nucl. Structure," Kingston 1960, eds. D. A. Bromley and E. W. Vogt (Univ. of Toronto Press and North-Holland, Amsterdam, 1960); A. Bohr, in "Int. Nucl. Physics Conf.," Gatlinburg 1966, eds. R. Becker, C. Goodman, P. Stelson and A. Zucker (Academic Press, New York, 1967).
2. R. Pitthan and Th. Walcher, Phys. Lett. 36B, 563 (1971); Z. Naturforsch. 27a, 1683 (1972).
3. M. B. Lewis, Phys. Rev. Letters 29, 1257 (1972); M. B. Lewis and F. E. Bertrand, Nucl. Phys. A196, 337 (1972).
4. L. Meitner, O. Hahn, and F. Strassmann, Z. Physik 106, 249 (1937).
5. T. Bar-noy and R. Moreh, Nucl. Phys., A229, 417 (1974).
6. G. M. Gurevich, L. E. Lazareva, V. M. Mazur, G. V. Solodukhov, and B. A. Tulupov, Nucl. Phys., A273, 326 (1976).
7. A. Veyssière, H. Beil, R. Bergère, P. Carlos, A. Leprêtre, and K. Kernbath, Nucl. Phys., A199, 45 (1973).
8. J. T. Caldwell, E. J. Dowdy, B. L. Berman, R. A. Alvarez, P. Meyer, Los Alamos Scietific Laboratory Report LA-UR76-1615, quoted in Lawrence Livermore Laboratory Report UCRL-78482, Atlas of Photoneutron Cross Sections Obtained with Monoenergetic Photons, ed. B. L. Berman.
9. M. B. Lewis and D. J. Horen, Phys. Rev., C10, 1099 (1974).

10. E. Wolynec, M. N. Martins and G. Moscati. Phys. Rev. Letters, 37, 585 (1976).

11. R. Pitthan, Z. Physik 260, 283 (1973).

12. R. Pitthan, F. R. Buskirk, E. B. Dally, J. N. Dyer and X. K. Maruyama, Phys. Rev. Lett. 33, 849 (1974) and Phys. Rev. Lett. 34, 848 (1975).

13. G. L. Moore, F. R. Buskirk, E. B. Dally, J. N. Dyer, X. K. Maruyama and R. Pitthan, Z. Naturforsch. 31a, 668 (1976).

14. R. Pitthan, F. R. Buskirk, E. B. Dally, J. O. Shannon and W. H. Smith, submitted to Phys. Rev. C.

15. C. R. Fischer and G. H. Rawitscher, Phys. Rev. 135B, 377 (1964).

16. C. W. de Jager, H. de Vries and C. de Vries, Atomic Data and Nuclear Data Tables 14, 479 (1974).

17. S. T. Tuan, L. E. Wright, D. S. Onley, Nucl. Instr. Meth. 60, 70 (1968).

18. J. F. Ziegler and G. A. Peterson, Phys. Rev. 165, 1337 (1968).

19. R. S. Hicks, I. P. Auer, J. C. Bergstrom and H. S. Caplan, Nucl. Phys. A278, 261 (1977).

20. E. S. Ginsberg and R. H. Pratt, Phys. Rev. 134B, 849 (1964).

21. E. F. Gordon and R. Pitthan, Nucl. Instr. Methods, in press.

22. J. Weneser and E. K. Warburton, in "The Role of Isospin in Nuclear Physics," edited by D. H. Wilkinson (North-Holland, Amsterdam, 1969).

23. A. Schwierczinski, R. Frey, E. Spamer, H. Theissen and Th. Walcher, Phys. Lett. 55B, 171 (1974).

24. D. H. Youngblood, J. M. Moss, C. M. Rozsa, J. D. Bronson, A. D. Bacher and D. R. Brown, Phys. Rev. C13, 994 (1976).

25. M. Danos, Nucl. Phys. 5, 23 (1958).

26. K. F. Liu and G. E. Brown, Nucl. Phys. A265, 385 (1976).

27. I. Hamamoto, in "Proc. of the Int. Conf. on Nuclear Structure Studies Using Electron Scattering and Photoreaction," Sendai, 1972; eds. K. Shoda and H. Ui (Suppl. Res. Rep. Lab. Nucl. Sci., Tohoku Univ., Vol. 5, 1972).

28. N. Auerbach and A. Yeverechyahu, Ann. Phys. (N.Y) 95, 35 (1975).

DEPARTMENT OF THE NAVY

Dept. of Physics & Chemistry
Attn: Code 61Pt
Naval Postgraduate School
Monterey, California 93940

OFFICIAL BUSINESS
PENALTY FOR PRIVATE USE, $300

POSTAGE AND FEES PAID
DEPARTMENT OF THE NAVY
DoD 316

U.S.MAIL

DR.XAVIER K. MARUYAMA
NAT.BUR.STANDARDS
CENTRE F.RAD.RES.
WASHINGTON DC 20234